

See discussions, stats, and author profiles for this publication at: <https://www.researchgate.net/publication/231701286>

# Direct Observation on the Surface Fracture of Ultrathin Film Double-Network Hydrogels

ARTICLE *in* MACROMOLECULES · MARCH 2011

Impact Factor: 5.8 · DOI: 10.1021/ma2000527

---

CITATIONS

19

---

READS

41

6 AUTHORS, INCLUDING:



Zi Liang Wu

Zhejiang University

29 PUBLICATIONS 459 CITATIONS

SEE PROFILE

# Direct Observation on the Surface Fracture of Ultrathin Film Double-Network Hydrogels

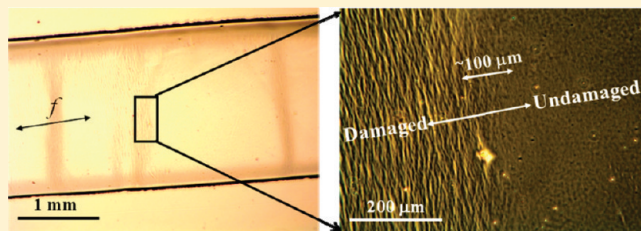
Songmiao Liang,<sup>†,‡</sup> Zi Liang Wu,<sup>†</sup> Jian Hu,<sup>†</sup> Takayuki Kurokawa,<sup>‡,§</sup> Qiu Ming Yu,<sup>†</sup> and Jian Ping Gong<sup>\*,‡</sup>

<sup>†</sup>Graduate School of Science, Hokkaido University, Sapporo 060-0810, Japan

<sup>‡</sup>Faculty of Advanced Life Science, Hokkaido University, Sapporo 060-0810, Japan

<sup>§</sup>Creative Research Initiative Sousei, Hokkaido University, Sapporo 001-0021, Japan

**ABSTRACT:** Double-network (DN) hydrogels have attracted much attention in the soft matter community due to their excellent mechanical performance and unique fracture mechanism. On the basis of ultrathin film technique and optical microscope, we here report a method which is quite effective for accessing the fractured microstructure of DN hydrogels formed during the tensile and tearing process. During tensile deformation, fracture of the first network occurs even before yielding occurs. Concomitant with the yielding, wrinkle-like structure, which is due to the fracture of the first network, is clearly observed for the first time. This wrinkle-like structure disappears upon further deformation to strain-hardening region because of the further fracture of the first network. Similar microstructures are observed at the crack tip for samples experienced the tearing test. This work provides direct proofs for the assumption concerning the occurrence of local yielding and the formation of a huge damage zone at the crack tip during the crack propagation process of DN hydrogels.



## INTRODUCTION

The double-network (DN) technique has been developed by our group with an emphasis on addressing the poor mechanical properties of polymer hydrogels since 2003.<sup>1</sup> DN gels, composed of a rigid and brittle first network and a soft and ductile second network, show not only a high fracture stress and strain but also a high toughness with a fracture energy ( $G$ ) of  $10^2$ – $10^3$  J/m<sup>2</sup>, which is 10–1000 times larger than that of the individual single-network hydrogels.<sup>2–4</sup> Owing to the tough feature, extensive studies have been focused on the toughening mechanism of this soft and water containing wet material.<sup>3–12</sup> Investigations on the tensile test have revealed the necking phenomena and the large hysteresis of the DN gels, implying that the DN gels could accumulate the internal damage before its macroscopic fracture through the connection of the soft second network to the fragments of the brittle first network.<sup>5,9</sup> As a result, softening of the gels occurs concomitantly with large energy dissipation. This dissipation in the energy is considered to be active at the crack tip and contributes dominantly to the high tearing energy.<sup>5,6,8</sup> Phenomenological models concerning the formation of the softened (damaged) zone at the crack tip vicinity and its role to the propagation of the crack tip have been proposed.<sup>6,8</sup> According to these models, the softened damage zone was estimated in an order of hundreds of micrometers. This softening of the fractured surface has been clarified by the micromechanical measurement using AFM.<sup>11</sup> Furthermore, direct visualization of the crack tip using 3D violet laser scanning microscopy confirmed the existence of the damage zone of several hundred

micrometers, which seems to be several times wider than the model prediction.<sup>12</sup> However, those previously developed methods give no detailed information on the characteristic structure distribution of the damage zone. Main blocks to the issues arise from the high water content and the large thickness of the bulk DN gels, which lead to an average overlay of the characteristic structure along the observed direction. Consequently, magnification and resolution on the characteristic structure were very limited.

More recently, we have successfully created the ultrathin film DN (UTDN) gels of 100  $\mu$ m in thickness by coupling the salt-controlled swelling process and the polymer chain preinforced technique.<sup>13</sup> These UTDN gels show very high toughness which is comparable with that of the bulk DN gels. Yielding and necking behavior have also been observed in these gels during the tensile process. These results indicate that the DN technique was effective even at the micrometer scale by means of a similar toughening mechanism. This permits us to further study about the fracture structure of the DN gels using the UTDN gels, which takes great advantage of removing the thickness and water interference suffered by the bulk DN gels. In this work, we report the visualization of the characteristic fracture structure of the UTDN gels induced by tensile and/or tearing process and discuss the correlation of these two processes.

**Received:** January 13, 2011

**Revised:** February 24, 2011

**Published:** March 17, 2011

## EXPERIMENTAL SECTION

**Materials.** 2-Acrylamido-2-methylpropanesulfonic acid (AMPS; Toagosei Co., Ltd.) was used as received. Acrylamide (AAm; Junsei Chemical Co. Ltd.) and *N,N'*-methylenebis(acrylamide) (MBAA; Tokyo Kasei Co., Ltd.) were recrystallized from chloroform and ethanol, respectively, before use. 2-Oxoglutaric acid (OA; Wako Pure Chemical Industries, Ltd.), a radical initiator for the gelation reactions, was used as received. Milli-Q (18.2 M $\Omega$  cm) water was used in all experiments.

**Synthesis of the UTDN Gels.** In terms of our previous work, the procedure for synthesizing the ultrathin film poly(2-acrylamido-2-methylpropanesulfonic acid)/polyacrylamide (PAMPS/PAAm) double-network (UTDN) gels was performed by multistep UV-light-initiated polymerization (UVIP).<sup>13</sup> Using two glass plates spaced with 50  $\mu$ m polyethylene film, we first created the ultrathin PAMPS gels by the UVIP, where 2-acrylamido-2-methylpropanesulfonic acid (1 mol/L, Tokyo Kasei, Japan) was used as monomer and *N,N'*-methylenebis(acrylamide) (0.04 mol/L, Tokyo Kasei, Japan) was used as cross-linking agent with an initiator of 2-oxoglutaric acid (OA) (0.001 mol/L, Wako, Japan). Then, the PAMPS gels were immersed in acrylamide (AAm) (4 mol/L, Wako, Japan)/OA ( $1.67 \times 10^{-4}$  mol/L) aqueous solution, containing 0.08 mol/L NaCl, to obtain a controlled-swelling state. Following this step, another UVIP to the partially swelled PAMPS gels was performed to *in situ* introduce PAAm chains to the PAMPS network. Finally, the mechanically enhanced PAMPS gels were washed until free from NaCl by pure water. They were then immersed in AAm (2 mol/L)/OA ( $1.67 \times 10^{-4}$  mol/L) solution for 10 h, and the UVIP was applied to obtain the UTDN gels. The obtained UTDN gels were stored and fully swelled in water for the next experiments. The thickness of the fully swelled UTDN gels is  $100 \pm 10$   $\mu$ m.

**Mechanical Test of the UTDN Gels.** Tensile mechanical properties of the UTDN gels were measured with a commercial test machine (Tensilon RT-1150A, Orientec Co.) in air. The samples were cut into a dumbbell shape standardized as JIS-K6251-7 sizes (length 51 mm, width 4 mm, gauge length 20 mm) with a gel cutting machine (Dumbbell Co., Ltd.). The sample length between two clamps was  $\sim 30$  mm. The stress–strain curves were recorded while the sample gel was stretched at a constant rate of 40 mm/min. The tearing test was performed in air using the above machine in mode III test. The UTDN gels were cut into the shape, which has the standardized JIS-K6252 1/2 sizes (thickness (*w*)  $100 \pm 10$   $\mu$ m, width (*d*) 7.5 mm, length (*l*) 50 mm, the length of the initial notch is 20 mm), with a gel cutting machine (Dumbbell Co., Ltd.). The two arms of the test sample were clamped, and the one was pulled upward at a velocity *V*, while the other was maintained stationary. The tearing force *F* was recorded. *G* is calculated by dividing the average of *F* at steady state during tearing by the gel thickness.<sup>2–4</sup> The tearing velocity *V* was set at the range of 10–100 mm/min.

**Microscopic Observation of the UTDN Gels.** Samples for the microscopic observation of tearing-induced fracture and tensile-induced fracture were shaped the same as that for the above tearing test and the tensile test, respectively. For observation of the tensile-induced fracture structure, the samples were first experienced to a designated prestrain under the tensile velocity of 40 mm/min. The samples for microscopic observation of the tearing-induced fracture structure were first experienced to a pretearing treatment (tearing distance 10 mm) under the tearing velocity of 40 mm/min. Prior to the microscopic observation, all of the prepared samples were then relaxed and reswelled in distilled water. Observation of the fracture structure was performed by a phase contrast optical microscope (Olympus CKX41) equipped with  $\times 5$  and  $\times 20$  objective lens at the free-standing state of the samples. For a comparison, the tearing-induced damage zone of the UTDN gels was also observed using a 3D violet laser scanning microscope (VK-8700, KEYENCE Co., Ltd.) according to our previous work.<sup>12</sup> Moreover, the samples for *in situ* yielding observation were shaped as that for the tensile test above. Yielding process of the samples under the stretching rate

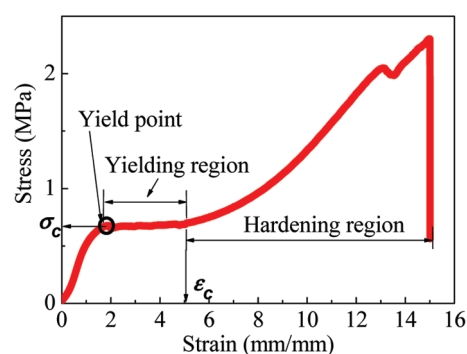


**Figure 1.** Stress–strain curve of the ultrathin film DN gel (thickness:  $100 \pm 10$   $\mu$ m).

of 40 mm/min was then *in situ* monitored by a polarized optical microscope (Nikon LV100POL) equipped with  $\times 5$  objective lens and 530 nm tint plate. The sample was stretched in the direction  $45^\circ$  to the polarized optical direction. Periodicity of the wrinkle-like pattern of the optical images was analyzed by Image J software.

## RESULTS AND DISCUSSION

**Stress–Strain Behavior of the UTDN Gels.** Figure 1 presents the typical stress–strain curve of the UTDN hydrogels. Three characteristic regions, consisting of the preyielding region, yielding region, and strain-hardening region, are observed for the UTDN gel, similar to that of bulk DN hydrogels.<sup>5</sup> As has been clarified in our previous work, in the preyielding region, the stress is mainly sustained by the densely cross-linked polyelectrolyte PAMPS network.<sup>14</sup> Beyond the yielding point, the yielded zone appears along with the break of the PAMPS network and the further elongation of the PAAm coils. This process is crucial to the toughening of the DN network because of the successive damage accumulation of the first brittle network. High energy dissipation and softening of the DN gels are concomitant with this process. We have observed that the average strain width of the yielding region for the UTDN gels is about 300%, which is smaller than  $\sim 400\%$  of the bulk DN gels prepared at a similar condition. Moreover, the strain-hardening region starts at a strain about 500%. This may imply that the PAAm coils need about 500% strain before exceeding the critical yielding stress. The hardening region of the DN gels arises from the highly stretching of the PAAm network under the further external loading.

**In Situ Observation of Yielding Process.** To investigate the growth of the yielded zone, we have *in situ* tracked the yielding process by polarized optical microscope (POM) observation. One of the most key factors in this observation is inserting of a 530 nm tint plate in the polarized optical microscope. The tint plate can sensitively indicate the molecular orientation induced by tensile deformation through a fixed color-band shift. Figure 2 shows the POM images during the yielding process of the UTDN gels. Two distinct color domains, blue (1) and purple (2), are observed for the samples in the yielding region. Blue domain is the yielded zone with high molecular orientation aligning to the stretching direction, while purple domain denotes the one where the yielding did not happen with low molecular orientation. Around the yielding point in Figure 1, the blue domain starts to appear (Figure 2a), corresponding to the starting of yielding zone. With the increase of the applied strain, the blue domain increases (Figure 2b,c) and develops to the whole sample (Figure 2d) at the strain where the yielding region finishes in Figure 1.



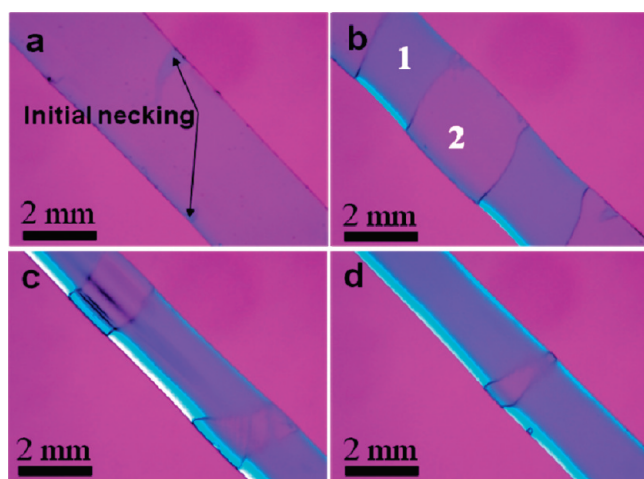


**Figure 2.** Structure change during the yielding process of the ultrathin film DN gels at the strain of 150% (a), 250% (b), 350% (c), and 450% (d) *in situ* monitored by the polarized optical microscope equipped with a 530 nm tint plate. The sample was stretched in the direction 45° to the polarized optical direction. During the yielding process, the undamaged zone (purple region) and damaged zone (blue region) coexist.

Further, we also employ this method to observe the stretching process of pure PAAm network that has a negative birefringence. With the same crossover angle, blue color which arises from the molecular orientation of the PAAm network along the stress direction was also observed. It becomes deeper and deeper with the increase of the applied strain (data not shown). This result clarified that the blue domain in the UTDN gels was mainly due to the orientation of the PAAm network. This is in agreement with the argument that in the yielding region PAAm chains sustain the load and are in highly stretched state. It should be noted that the PAAm network was dominantly abundant in the composition of the DN gels. The molar ratio between the PAMPS network and the PAAm network was about 1:20 for bulk DN gel. A similar composition was expected in the UTDN gels. Accordingly, the birefringence from the orientation of the PAMPS network is weaker and negligible compared with that of PAAm network.

**Characteristic Fracture Structure of the UTDN Gels.** To clarify the fracture structure of the PAMPS network in the yielding region, we further observed the characteristic fracture structure of the UTDN gels by phase contrast microscope at high magnification, and the results are presented in Figure 3. These images were obtained from the free-standing state of the gels after suffered to a designated prestrain and reswelling in water. In the preyielding region, smooth surface was observed, and there was no characteristic structure under the microscopic scale (Figure 3a). This is in agreement with the fact that under the low prestrain of 100% the PAMPS network is strong enough to resist the applied stress and remains almost undamaged. In both the yielding point and the necking region, we found that the applied prestrain can induce the formation of interesting anisotropic fracture structure in the UTDN gels. Figure 3b illustrates a wrinkle-like fracture structure of the UTDN gels formed under a prestrain of 200% (at yielding point). The wrinkles were mutually connected with very high aspect ratio even though the wrinkle-like character is not quite obvious. The characteristic direction  $f$  of the wrinkles is vertical to the direction of the applied stress  $F$ , suggesting a parallel and gradient fracture of the PAMPS

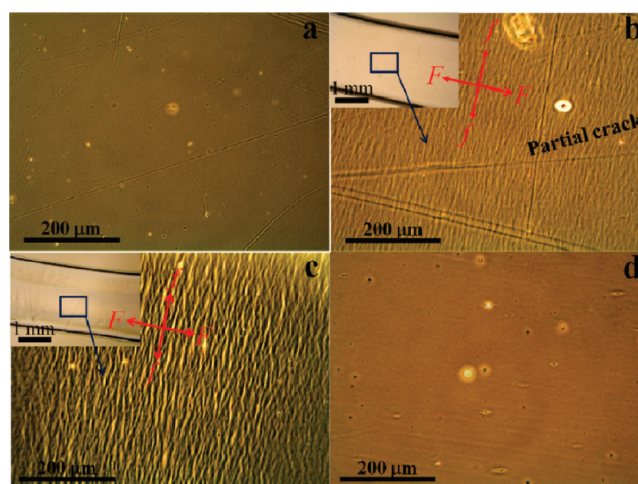


**Figure 3.** Phase contrast microscope images of the ultrathin film DN gels at the free-standing state after suffered to a prestrain of 100% (a), 200% (b), 300% (c), and 800% (d).  $F$  and  $f$  denote the direction of the tensile force and the wrinkle-like damage patterns, respectively. Micro-crack was observed as shown by the arrows in (b). Inserted images in (b) and (c) are in low magnification. The observation was performed on samples reswelled in water after tensile deformation.

network along the stretching direction. With the further increase of the applied prestrain, the wrinkle-like fracture structure developed and became distinct due to the persistent fracture of the PAMPS network. In the hardening region, however, the wrinkle-like structure disappeared (Figure 3d). This result indicates that by applying the high prestrain of 800%, highly stretching of the DN gels at the hardening region could result in further fracture of the PAMPS network which possibly produces smaller PAMPS clusters beyond the observation scale. These results indicate that irreversible damage of the PAMPS network occurs in both the yielding region and hardening regions.

The anisotropic structure observed here seems in agreement with the small-angle neutron scattering (SANS) observation, which indicates that a tensile deformation of a bulk DN gel at the tensile strain of  $\sim 50\%$  results in periodic and mesoscale ( $1.5\ \mu\text{m}$ ) compositional fluctuations in both PAMPS and PAAm along the stretched direction.<sup>17</sup> However, the characteristic period of these wrinkles is averaged at about  $7\ \mu\text{m}$ , which is larger than the periodicity observed by the neutron scattering of bulk DN gels.

This result confirms explanation of the fracture accumulation in the necking region.<sup>5</sup> It was assumed that in the course of necking deformation the first PAMPS network fragments into small clusters, and the clusters play a role of cross-linker of long PAAm chains (see Figure 4, ref 5) because the cross-linker concentration of the second network is so slight.<sup>5</sup> However, the anisotropic wrinkle-like fracture structure as well as the SANS results indicates that PAMPS is fractured into clusters anisotropically. Accordingly, the illustration of fracture structure shown in Figure 4 of ref 5 needs modification.

In the previous study, it has been assumed that the high tearing energy of the DN gels was owing to the presence of the local yielding, which behaves similarly for the energy dissipation as that shown in the tensile process. Using the phase contrast microscope and a 3D violet laser scanning microscope, we have investigated the characteristic structure of the damage zone at the crack front vicinity of the UTDN gels. A smooth crack surface was observed (Figure 4a). As shown by the phase contrast

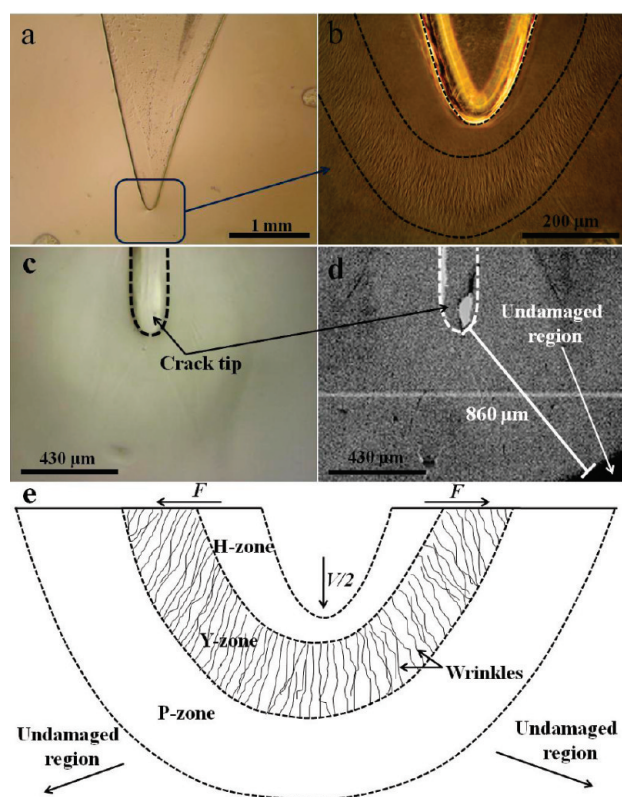


**Figure 4.** Tearing-induced fracture structure at the crack tip of the ultrathin film DN hydrogel. (a) Photo image of the crack tip. (b) Damaged zone observed by a phase contrast microscope. (c, d) The same damaged zone observed by a 3D violet laser scanning microscope with reflection mode ((c) optical image, (d) high-low image). (e) A sketch of the tearing-induced fracture structure. The damage zone observed in (d) is due to the scattering of light by the inhomogeneous structure beneath the surface of the damage zone. The damage zone can be divided into three subzones according to their characteristic surface structure. The observation was performed for samples reswelled in water after the tearing test.

microscope in Figure 4b, under a high magnification, the damage zone of  $\sim 300 \mu\text{m}$  was observed at the crack front with very clear boundary. The damage zone was composed of two different regions. One region was characterized with homogeneously distributed and mutually connected wrinkle-like structure, similar to that observed in the tensile-induced yielding region (Figure 3c). Furthermore, the wrinkle in this region was parallel to the propagation direction of the crack, while vertical to the loading stress. This morphological feature also well agreed with that observed in the tensile-induced yielding region (Figure 3c). So we named this region as Y-zone (yielding). In contrast, no special structure, under the observation scale, was observed in the region that was located close to the fractured surface. As this region had experienced a higher deformation than the Y-zone, it should correspond to the tensile-induced hardening region in Figure 3c. So we named this region as H-zone (hardening).

The average thickness of H-zone is about one-third to that of Y-zone. Such structure difference can be attributed to the stronger damage of PAMPS network in H-zone than that in Y-zone due to the highly local strain gradient developed in the crack front vicinity. Combined with the results shown in Figure 3c,d, during the tearing process, local strain suffered by

H-zone and Y-zone should correspond to that for the hardening region and the yielding region, respectively. These results again experimentally testify the assumption that states the presence of the local yielding at the crack front during the tearing process.<sup>12</sup>

Previous study has shown that the damage of the first polyelectrolyte (PAMPS) network occurs even at very small strain, in the preyielding region.<sup>9</sup> Therefore, fracture of PAMPS should also occur in front of the Y-zone. However, using the phase contrast microscope, we could not detect this structure change, as shown in Figure 3a. However, this region can be clearly observed by using 3D laser scanning microscope system, as has been demonstrated in our previous work.<sup>12</sup> The high–low image mode of the 3D laser microscopy can sensitively detect the polymer density fluctuation based on the reflection of laser light in the gel. For a damaged gel sample reswelling with water, the heterogeneity of the sample increased, which favors the scattering of the laser (details were described in the Appendix of ref 12).

As seen in Figure 4d, compared with the results observed by the phase contrast microscope, a much wider damage zone is observed by using 3D laser microscopy, and the measured thickness of the damage zone in the UTDN gel is about  $860 \mu\text{m}$ , which is almost 3 times larger than the total thickness of Y-zone and H-zone. This result implies that, except for the observed Y-zone and H-zone, a wide damage zone, which corresponds to the preyielding region (Figure 1), also exists in the crack front vicinity. We called here this region as P-zone, which is about 2 times as wide as Y-zone + H-zone. The damage accumulation could thus happen not only in the yielding region/local yielding region but also in the preyielding region and hardening region.

According to the previous study, the effective fracture energy  $G$  consists of the intrinsic fracture energy of the damaged gel  $G_0$  and a dissipation term representing the formation of the damage zone.<sup>8</sup> Assuming that (i) the highly stretched region ahead of the crack tip becomes a softer damaged material at  $\sigma_c$  and (ii) the local yielding behavior is almost identical to the macroscopic necking in tensile tests, the dissipation term by the damage zone is given by  $k\sigma_c\epsilon_ch$ , where  $k$  is the geometrical factor and  $\epsilon_c$  is the strain of the damage zone before hardening at a yielding stress  $\sigma_c$ . Since  $k\sigma_c\epsilon_ch \gg G_0$

$$G \approx k\sigma_c\epsilon_ch \quad (1)$$

The linear relation between  $G$  and  $h$  has been confirmed experimentally in our previous study on the bulk DN gels, whereupon the damage zone thickness  $h$  was determined by using the 3D violet laser scanning microscope system.<sup>12</sup> However, the ratio of  $G/h$  was found to be  $0.91 \times 10^6 \text{ J/m}^2$ , about 6 times smaller than the value of  $\sigma_c\epsilon_c$  estimated from the tensile test. This large discrepancy was attributed to three possible reasons, that is, (1) overestimation of the  $h$  value by the 3D laser scanning method, (2) surface effect, and (3) swelling of the sample after yielding. The results obtained in Figure 4 show that the damage zone formed in the preyielding region (P-zone) is about 2 times wider than the sum of yielding (Y-zone) and hardening region (H-zone). Since the damage accumulation of the first polyelectrolyte (PAMPS) network in the preyielding region is much smaller than the two other regions, the  $h$  value determined by the 3D laser scanning method is an overestimation for the eq 1. That is, possibility (1) might be the main reason for this large discrepancy. To confirm this, we further investigated the fracture energy  $G$  and damage zone thickness of a UTDN gel. Instead of the overall damage zone thickness  $h = P + Y + H$ , we plot the tearing energy ( $G$ ) of the UTDN gels



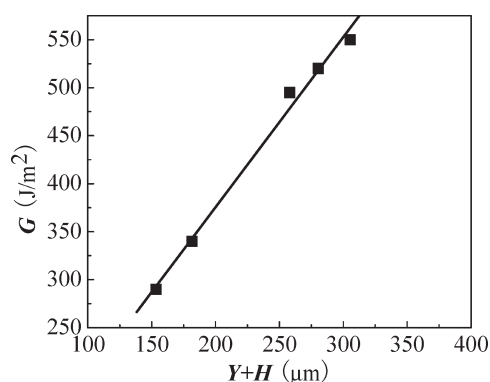


**Figure 5.** Relationship between the tearing energy ( $G$ ) and the thickness of the damage zone ( $Y + H$ ). The different  $G$  and  $Y$ ,  $H$  were measured for an ultrathin film DN gel with various tearing velocity.

obtained from different tearing velocity against the damage zone thickness due to yielding and hardening, ( $Y + H$ ). As a result, a linear relationship between  $G$  and ( $Y + H$ ) is observed, as shown in Figure 5. The ratio between  $G$  and  $Y + H$  estimated from the slope of the linear line,  $G/(Y + H)$ , is about  $1.72 \times 10^6 \text{ J/m}^2$ . This value is half of  $\sigma_c \varepsilon_c \approx 3.4 \times 10^6 \text{ J/m}^2$ , as estimated from the tensile result shown in Figure 1. A factor of 2 can be explained by the reswelling of the gel after prestrain. That is, considering the swelling degree change of the damaged DN gel, eq 1 is confirmed by the experimental observation, where  $h$  is the sum thickness of Y-zone and H-zone.

## CONCLUSIONS

Combining the ultrathin film technique with optical microscope, we are able to simultaneously observe the deformation process and the structure change *in situ* of ultrathin film DN gels. During the tensile deformation of the gels, coexistence of the yielding and unyielding domains is clearly observed by the strong color contrast, which is originated from the difference in the molecular orientation in these domains. Three characteristic damage zones, P-zone, Y-zone, and H-zone, arose from the highly local strain gradient corresponding to the preyielding, yielding, and hardening, respectively, were observed in the vicinity of crack tip. The wrinkle-like structure, whose characteristic direction was vertical to the direction of the applied stress, was clearly observed in the Y-zone as well as in the yielding region of the sample in tensile deformation for the first time, indicating the anisotropic fracture and structure change of the gel. The very diffuse preyielding zone, though its contribution in dissipating the fracture energy is small, might be important in further lowering the stress concentration at the crack tip in addition to that by the yielding zone. This result, in addition to our previous results, further confirms that the extraordinarily high toughness (high tearing energy) of the DN gels is attributed to the formation of the sub-millimeter scale, huge local damage zone at the crack tip during the crack propagation. The methods reported here are useful not only for further understanding the toughening mechanism of the DN gels but also for investigating the crack propagation of the other polymer gels.

## AUTHOR INFORMATION

### Corresponding Author

\*E-mail: gong@mail.sci.hokudai.ac.jp.

### Present Addresses

<sup>†</sup>Vontron Technology Co., Ltd., Beijing, 102249, China.

## ACKNOWLEDGMENT

This research was financially supported by a Grant-in-Aid for Specially Promoted Research (No. 18002002) from the Ministry of Education, Science, Sports and Culture of Japan.

## REFERENCES

- (1) Gong, J. P.; Katsuyama, Y.; Kurokawa, T.; Osada, Y. *Adv. Mater.* **2003**, *15*, 1155.
- (2) Tanaka, Y.; Kuwabara, R.; Na, Y. H.; Kurokawa, T.; Gong, J. P.; Osada, Y. *J. Phys. Chem. B* **2005**, *109*, 11559.
- (3) Tsukeshiba, H.; Huang, M.; Na, Y. H.; Kurokawa, T.; Kuwabara, R.; Tanaka, Y.; Furukawa, H.; Osada, Y.; Gong, J. P. *J. Phys. Chem. B* **2005**, *109*, 16304.
- (4) Huang, M.; Furukawa, H.; Tanaka, Y.; Nakajima, T.; Osada, Y.; Gong, J. P. *Macromolecules* **2007**, *40*, 6658.
- (5) Na, Y. H.; Tanaka, Y.; Kawauchi, Y.; Furukawa, H.; Sumiyoshi, T.; Gong, J. P.; Osada, Y. *Macromolecules* **2006**, *39*, 4641.
- (6) Brown, H. R. *Macromolecules* **2007**, *40*, 3815.
- (7) Shull, K. R. *J. Polym. Sci., Part B: Polym. Phys.* **2006**, *44*, 3436.
- (8) Tanaka, Y. *Europhys. Lett.* **2007**, *78*, S6005.
- (9) Webber, R. E.; Creton, C.; Brown, H. R.; Gong, J. P. *Macromolecules* **2007**, *40*, 2919.
- (10) Miquelard-Garnier, G.; Demoures, S.; Creton, C.; Hourdet, D. *Macromolecules* **2006**, *39*, 8128.
- (11) Tanaka, Y.; Kawauchi, Y.; Kurokawa, T.; Furukawa, H.; Okajima, T.; Gong, J. P. *Macromol. Rapid Commun.* **2008**, *29*, 1514.
- (12) Yu, Q. M.; Tanaka, Y.; Furukawa, H.; Kurokawa, T.; Gong, J. P. *Macromolecules* **2009**, *42*, 3852.
- (13) Liang, S.; Yu, Q. M.; Yin, H.; Wu, Z. L.; Kurokawa, T.; Gong, J. P. *Chem. Commun.* **2009**, 7518–7520.
- (14) Nakajima, T.; Furukawa, H.; Tanaka, Y.; Kurokawa, T.; Osada, Y.; Gong, J. P. *Macromolecules* **2009**, *42*, 2184.
- (15) Oeser, R.; Picot, C.; Herz, J. *Polymer Motions in Dense Systems*; Richter, D.; Springer, T., Eds.; Springer-Verlag: Berlin, 1988; p 104.
- (16) Mendes, E.; Lindner, P.; Buzier, M.; Boué, F.; Bastide, J. *Phys. Rev. Lett.* **1991**, *66*, 1595.
- (17) Tominaga, T.; Tirumala, V. R.; Lin, E. K.; Gong, J. P.; Furukawa, H.; Osada, Y.; Wu, W. L. *Polymer* **2007**, *48*, 7449–7454.